Available online at www.sciencedirect.com

ScienceDirect

MATTER AND RADIATION AT EXTREMES

Matter and Radiation at Extremes 1 (2016) 114–122

www.journals.elsevier.com/matter-and-radiation-at-extremes

Research article

Dynamics of N^{5+}-H electron capture in Debye plasmas

L. Liu*, J.G. Wang

Data Center for High Energy Density Physics, Institute of Applied Physics and Computational Mathematics, P. O. Box 8009-26, Beijing, 100088, People's Republic of China

Received 15 October 2015; revised 15 January 2016; accepted 25 February 2016
Available online 26 March 2016

Abstract

The electron capture in N^{5+}-H collisions imbedded in a Debye plasma is studied by using the two-center atomic orbital close-coupling method in the energy range from 1 keV/u to 200 keV/u. The atomic orbitals and electron binding energies of atomic states are calculated within the Debye–Hückel approximation of the screened Coulomb potential and used in atomic orbital close-coupling dynamics formalism to calculate the electron capture cross sections. The electron capture cross sections and the charge transfer spectral lines of $N^{4+}(1s^2nl)$ for a number of representative screening parameter values are presented and discussed. It is found that the screening of Coulomb interactions affects the entire collision dynamics and the magnitude and energy behavior of state-selective cross sections. The changes in electron binding energies and capture cross sections when the interaction screening varies introduce dramatic changes in the radiation spectrum of $N^{4+}(1s^2nl)$ capture states with respect to the unscreened interaction case.

PACS Codes: 34.70.$^+$e; 34.20.Cf; 52.20.Hv

Keywords: Electron capture; Debye plasma; Screening; Atomic orbital close-coupling

1. Introduction

Electron capture processes between atoms and multi-charged ions have been subject to extensive theoretical and experimental studies over the past five decades due to the important role in laboratory and astrophysical plasmas [1–5]. However, the atomic collision processes in the environments of hot dense plasmas have been investigated relatively scarcely, where the Coulomb interactions between charged particles may be significantly screened. To the best of our knowledge, the studies involving heavy-particle collision processes in hot, dense plasmas are those for proton-impact excitation of $n = 2$ fine-structure levels of hydrogenlike ions [6], electron capture in proton-hydrogenic ion collisions [7] in a Debye plasma by using the Bohr–Lindhard classical model, symmetric resonant charge exchange in hydrogenlike ion-parent nucleus collisions [8], and the classical trajectory Monte Carlo (CTMC) study of electron capture and ionization in hydrogen atom-fully stripped ion [9] and hydrogen atom-He-like ions [10] collisions. Quite recently, we have also performed extensive studies of the excitation, electron capture and ionization processes in H^+-H(1s) [11], He^{2+}-H(1s) [12–14] and O^{8+}-H(1s) [15] collision systems in a Debye plasmas by using the two-center atomic orbital close-coupling (TC-AOCC) method in the intermediate energy range. We would like to note that only the collision systems with one-electron and two heavy nuclei have been investigated in most of the above mentioned studies. The investigation of collision systems with multi-electron in hot dense plasma is very scarce. In Ref. [10], only the total charge transfer and ionization cross sections have been calculated for He-like

* Corresponding author.
E-mail address: liu_ling@iapcm.ac.cn (L. Liu).
Peer review under responsibility of Science and Technology Information Center, China Academy of Engineering Physics.

http://dx.doi.org/10.1016/j.mre.2016.03.001

systems (Li^+, Be^{2+}, B^{3+}, C^{4+}, N^{5+}, O^{6+}) and hydrogen atom collisions in Debye plasmas.

In the present work we shall study the electron capture process

$$N^{5+} + H(1s) \rightarrow N^{4+}\left(1s^2 nl\right) + H^+ \tag{1}$$

in a plasma by employing the two-center atomic orbital close-coupling (TC-AOCC) method in the energy range 1–200 keV/u. The interaction of an active electron with a stripped ion with charge Z in the plasma is represented by the Debye–Hückel potential (e is the unit charge)

$$V(r) = -\frac{Ze^2}{r} e^{-r/r_d} \tag{2}$$

where $r_d = (k_B T_e / 4\pi e^2 n_e)^{1/2}$ is the Debye screening length, T_e and n_e are the plasma electron temperature and density, respectively, and k_B is the Boltzmann constant. The representation of charged particle interaction in a plasma by the potential in Eq. (2) is adequate only if the Coulomb coupling parameter $\Gamma_c = e^2/(a k_B T_e)$ and plasma nonideality parameter $\gamma = e^2/(r_d k_B T_e)$ satisfy the conditions $\Gamma_c \leq 1$, $\gamma \ll 1$, where $a = [3/(4\pi n_e)]^{1/3}$ is the average interparticle distance. The atomic orbitals have been determined by variationally from the corresponding single-center Schrödinger equation with the potential in Eq. (2). In the N^{5+}-H collision system, the electron will be captured to the high principle quantum number n (around 4, 5) states of N^{4+} ion, so the use of a close-coupling method for description of its dynamics requires a very large expansion basis of atomic orbitals. In the present calculations, the target basis include all $n \leq 4$ bound states, while the basis centered on the projectile include all $n \leq 9$ ($l = 0$–5) bound states. The motivation of the present work is to study how the screened Coulomb interaction in Eq. (2) affects the dynamics of processes in Eq. (1) when the Debye screening length r_d varies. There have been many theoretical investigations in the past of process in Eq. (1) with pure Coulomb interactions between the particles. The semiclassical cross section calculations have been performed by using the perturbed stationary-state (PSS) [16] and molecular-orbital close-coupling (MOCC) [17–21] methods in the energy region 1–25 keV/u. In the intermediate and high energy regions, the classical trajectory Monte Carlo (CTMC) [5,22] (above 25 keV/u) and boundary corrected continuum intermediate state (BCCIS) methods [23] (above 50 keV/u) have also been used for the study of electron capture in this collision system.

The paper is organized as follows. In Sec. II we briefly outline the theoretical method used in the cross section and the charge transfer spectral line calculations. In Sec. III we present the results of cross section and charge transfer spectral line for process in Eq. (1) for different values of screening length r_d and analyze the effects of the screening on the dynamics of the process. In Sec. IV, we give our conclusions. Atomic units will be used throughout this paper, unless otherwise explicitly indicated.

2. Theoretical method

The TC-AOCC method is a standard method for describing the ion-atom collision processes at intermediate to high energies. The total scattering wave function is expanded over the traveling atomic orbitals centered on the projectile and the target and used in time-dependent Schrödinger equation to generate the coupled equations for the state amplitudes. The electronic states centered on each of the centers can be determined by using the even-tempered trial functions [24,25].

$$\chi_{klm}(\boldsymbol{r}; r_d) = N_l[\xi_k(r_d)] r^J e^{-\xi_k(r_d) r} Y_{lm}(\boldsymbol{r}) \tag{3}$$

$$\xi_k(r_d) = a\beta^k, k = 1, 2, \ldots N$$

where $N_l(\xi_k)$ is a normalization constant, $Y_{lm}(\boldsymbol{r})$ are the spherical harmonics, and α and β are variational parameters, determined by minimization of the energy. The atomic states $\Phi_{nlm}(\boldsymbol{r}; r_d)$ are then obtained as

$$\Phi_{nlm}(\boldsymbol{r}; r_d) = \sum_k c_{nk} \chi_{klm}(\boldsymbol{r}; r_d) \tag{4}$$

with the coefficients c_{nk} being determined by diagonalizing the single-center Hamiltonian. This diagonalization yields the energies $E_{nl}(r_d)$ of the bound states. The straight line approximation for the relative nuclear motion $R(t) = \boldsymbol{b} + \boldsymbol{v}t$ (b is the impact parameter and v is the collision velocity) is adopted. The total electron wave function Ψ can be expanded in terms of atomic orbitals in Eq. (4), each multiplied by a plane wave translational factor

$$\Psi(\boldsymbol{r}, t; r_d) = \sum_i a_i(t) \Phi_i^A(\boldsymbol{r}, t; r_d) + \sum_j b_j(t) \Phi_j^B(\boldsymbol{r}, t; r_d) \tag{5}$$

where the superscripts A and B designate the projectile (N^{5+}) and target (H), respectively. Inserting the Eq. (5) in the time dependent Schrödinger equation

$$\left[-\frac{1}{2}\nabla_r^2 + V_A(r_A) + V_B(r_B) - i\frac{\partial}{\partial t} \right] \Psi = 0 \tag{6}$$

where $V_{A,B}(r_{A,B})$ are the electron interactions with the target and projectile, respectively. $V_B(r_B)$ will be described by the Debye–Hückel potential

$$V_A(r_A) = -\frac{1}{r_A} e^{-r_A/r_d} \tag{7}$$

While for $V_A(r_A)$ we shall adopt the screened model potential

$$V_B(r_B) = \left(-\frac{Z_0}{r_B} + \frac{Z_1}{r_B} e^{-Z_3 r_B} + Z_2 e^{-Z_3 r_B} \right) e^{-r_B/r_d} \tag{8}$$

where $Z_0 = 5$, $Z_1 = -2$, $Z_2 = -13.351$ and $Z_3 = 9.7429$. These parameters in the above potential have been determined by a fitting procedure using the accurate potentials [26] for the Li-like ions. The r_d dependences of energies of 3l, 4l and 5l states of $N^{4+}(1s^2 nl)$ are shown in Fig 1. It can be seen from this

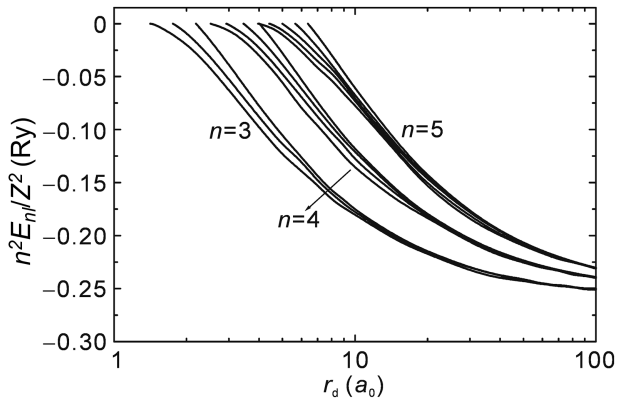

Fig. 1. r_d dependence of energies of 3l, 4l and 5l states of $N^{4+}(1s^2nl)$.

figure that in potential (8) the Coulomb degeneracy of l substates within a given n manifold is lifted and that with decreasing r_d the energy of atomic states decreases and eventually enters the continuum at certain critical Debye length. This implies that potential in Eq. (8) only supports a finite number of nondegenerate states for any finite value of r_d.

The first order coupled equations for the amplitudes $a_i(t)$ and $b_j(t)$ resulting from Eqs. (5) and (6) have the form

$$\begin{aligned} \mathrm{i}\left(\dot{\boldsymbol{A}}+\boldsymbol{S}\dot{\boldsymbol{B}}\right) &= \boldsymbol{H}\boldsymbol{A}+\boldsymbol{K}\boldsymbol{B} \\ \mathrm{i}\left(\dot{\boldsymbol{B}}+\boldsymbol{S}^{\dagger}\dot{\boldsymbol{A}}\right) &= \overline{\boldsymbol{K}}\boldsymbol{A}+\overline{\boldsymbol{H}}\boldsymbol{B} \end{aligned} \tag{9}$$

where $\boldsymbol{A}$ and $\boldsymbol{B}$ are the vectors of the amplitudes $a_i(t)$ and $b_j(t)$, respectively. $\boldsymbol{S}$ is the overlap matrix, $\boldsymbol{H}$ and $\overline{\boldsymbol{H}}$ are the $i\rightarrow i'$ and $j\rightarrow j'$ direct coupling matrices, and $\boldsymbol{K}$ and $\overline{\boldsymbol{K}}$ are the $i\rightarrow j$ and $j\rightarrow i$ electron exchange matrices. The coupled Eq. (9) are solved under the initial conditions

$$a_i(-\infty)=\delta_{1i}, b_j(-\infty)=0 \tag{10}$$

The electron capture cross section for the $1\rightarrow j$ transition is calculated as

$$\sigma_{cx,j}=2\pi\int_0^{\infty}\left|b_j(+\infty)\right|^2 b\mathrm{d}b \tag{11}$$

3. Results and discussion

As mentioned in Sec. I, all the $n \leq 9$ ($l = 0$–5) states of N^{4+} and $n \leq 4$ states of H have been included in expansion in Eq. (5) when solving the present coupled channel (Eq. (9)). We have performed the electron-capture cross section calculations for the N^{5+}-H collisions in the zero-screening case with the above basis set in the energy range 0.5–200 keV/u recently [27], and it was found that the results are convergent in the entire energy range studied. The total electron capture cross section agrees quite well (within 20%) with the experimental data [28,29] in the overlapping energy range. For the dominant electron capture channel $n = 4$, the AOCC cross section is about 25% larger than the experimental data of Ref. [28] and the MOCC data of Shimakura and Kimura [21], but agrees well with the MOCC results of Bendahman et al. [17] below 2.5 keV/u. For the subdominant channel $n = 3$, the AOCC results lie significantly below (one half) the experimental data of [28] in the energy range 0.8–7 keV/u.

Since the main goal of the present work is the study of electron capture dynamics with screened Coulomb interactions of Yukawa type, we need a convergence check of the results obtained by the adopted AO basis in the case of screened interactions. In Table 1 we compare the total cross sections for the collision energies of 10 keV/u and 100 keV/u calculated with basis sets containing all n $\leq$ 4 states on H and all states with $n \leq 8$, $n \leq 9$ and $n \leq 10$ ($l = 0$–5) centered on N^{4+} for $r_d = \infty$, $12a_0$, $6a_0$ and $2a_0$. We see that with the basis set containing all $n \leq 9$ states on N^{4+} the convergence of the results can be considered as being achieved for this energy for all considered values of the Debye length (to within 0.8%–5.6%), including also the unscreened case.

An insight into the dynamics of electron capture process in a Debye plasma can be obtained by analyzing the variation of electron exchange matrix element with r_d for different collision energies. As an example of the behavior of these matrix elements we show the R dependence of absolute values of $H(1s) \rightarrow N^{4+}(1s^2 3s)$ electron exchange elements (calculated for $E = 100$ keV/u) for the unscreened case and for the screening interactions with $r_d = 12a_0$, $6a_0$ and $2a_0$ in Fig. 2.

Table 1
Total electron capture cross sections (in units of 10^{-16} cm^2) in 10 keV/u and 100 keV/u N^{5+}-H collisions for the unscreened case ($r_d = \infty$) and for the screened cases with $r_d = 12a_0$, $6a_0$ and $2a_0$, calculated with basis sets containing all states with $n \leq 8$, $n \leq 9$ and $n \leq 10$ of N^{4+}, respectively.

E (keV/u)	r_d (a_0)	$n \leq 8$	$n \leq 9$	$n \leq 10$
10	Infinity	36.10981	35.77713	36.32037
	12	31.55507	32.19440	32.44888
	6	24.02691	24.93758	25.28270
	2	6.43744	5.49379	5.44393
100	Infinity	4.93946	5.26592	5.34452
	12	3.49838	3.26567	3.15171
	6	2.09284	1.94626	1.86593
	2	0.27387	0.22474	0.23819

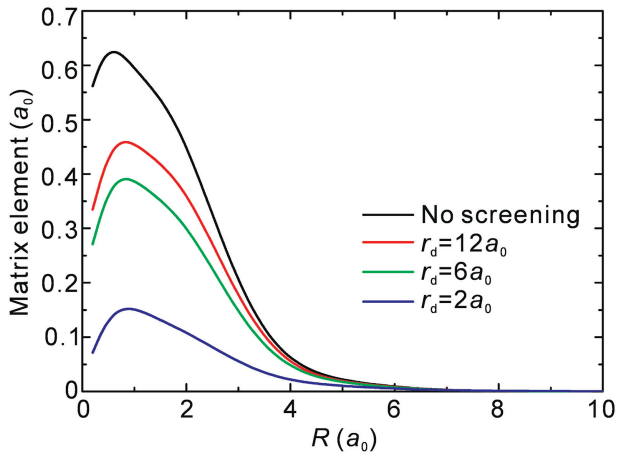

Fig. 2. Variation in absolute values of matrix element for $H(1s) \rightarrow N^{4+}(1s^2 3s)$ electron exchange transition for a number of r_d values and for the unscreened case.

We observe a significant reduction in the values of the matrix elements with decreasing r_d.

3.1. Electron capture cross sections with screened Coulomb interactions

We shall now investigate in more detail the energy behavior of partial cross sections for specific values of the Debye length. In order to illustrate the effects of the screening on the electron capture dynamics in the N^{5+}-H system, we choose the screening lengths $r_d = 12a_0$, $6a_0$, $4a_0$ and $2a_0$. In Fig. 3, we show the energy dependence of 3l state-selective cross sections for the unscreened case and for $r_d = 12a_0$, $6a_0$ and $2a_0$, respectively. The $n = 3$ electron-capture channel is the subdominant channel for this collision system in the unscreened case. From Fig. 3(b) we can see that the 3s cross sections for $r_d = 12a_0$ are larger than those of the unscreened case in the energy region below 10 keV/u, and the 3p and 3d cross sections do not differ much from those in the unscreened case. It should be noted in Fig. 3(c) that all 3l partial cross sections are significantly larger than the corresponding ones in the zero-screening case in the energy region below 30 keV/u. This is a consequence of the condition for strong interaction with the initial state is fulfilled for the 3l state due to the decrease of energy difference of $N^{4+}(1s^2 3l)$ and H(1s) states at this value of r_d. In fact, the 3l cross sections for $r_d = 4a_0$ attain the maximum in the considered energy region, which will be shown in the follows. Above 30 keV/u, the 3l cross sections for $r_d = 6a_0$ are a little smaller than those of the unscreened case due to the decrease of the coupling matrix with increasing the screening. Finally, Fig. 3(d) shows the 3s and 3p cross sections for $r_d = 2a_0$. For this value of r_d the 3d state is already in the continuum. It is worthwhile to note that in this case the magnitude of 3s capture cross section is larger than that of the other values of r_d and the unscreened case in the energy region below 3 keV/u. The magnitude of 3p cross section is smaller than the corresponding one in the zero screening case in the energy region below 2 keV/u, while for high energy range the 3p cross section become larger than that of the unscreened case. The relative magnitude of the 3l capture cross sections above 10 keV/u in all cases presented in Fig. 3 reflects the fact that the exchange coupling matrix elements for a given r_d are larger for larger l.

The energy dependence of 4l state-selective cross sections for the unscreened case and for $r_d = 12a_0$, $6a_0$ and $4a_0$ are shown in Fig. 4(a)–(d), respectively. The 4l electron-capture channel is the dominant channel for this collision system in the unscreened case. In Fig. 4(a) we see that the capture to the 4s states dominates up to 2 keV/u. Above this energy, the capture to the 4f state becomes dominant. It should be noted in Fig. 4(b) that the energy behavior and magnitude of 4l cross sections for the screened case with $r_d = 12a_0$ differ much from those in the unscreened case in the energy region below 20 keV/u. The 4s cross section in the zero screening case rapidly decrease with increasing the energy below 5 keV/u. In the case of interaction screening with $r_d = 12a_0$, the decrease becomes mild in the same energy region. This general behavior is also maintained for the 4p state. All 4l partial cross sections are significantly smaller than the corresponding ones in the zero screening case in the low energy region. This decrease is associated with the disappearance of the strong interaction zone on the internuclear distance due to the change of energy difference of $N^{4+}(1s^2 4l)$ and H(1s) states at this value of r_d and the small collision velocity. It should be noted in Fig. 4(c) that the 4l cross sections for $r_d = 6a_0$ are significantly different from those in the $r_d = 12a_0$ case, especially

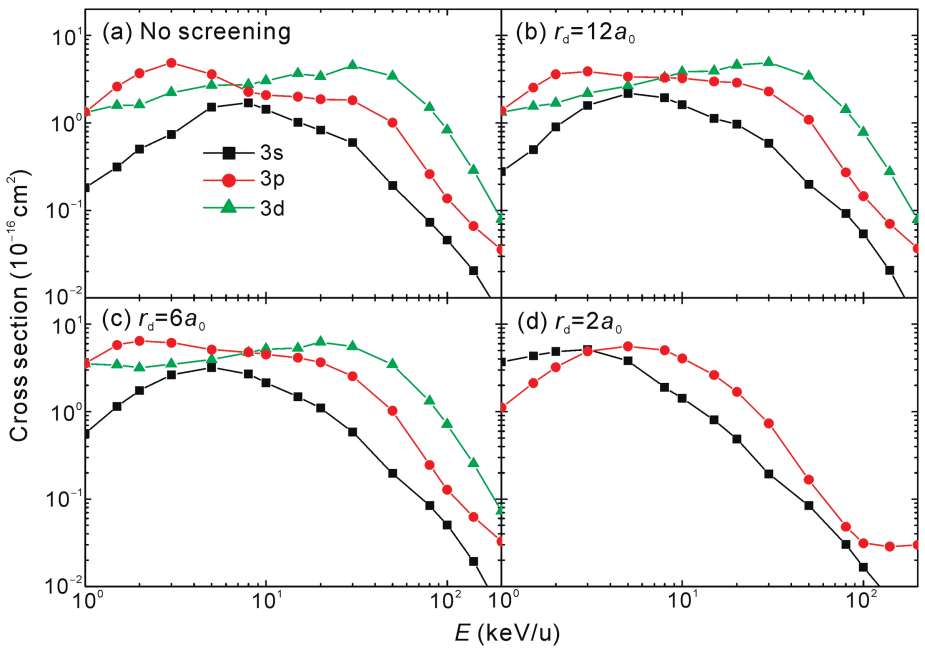

Fig. 3. Energy dependence of state-selective cross sections for electron capture to $N^{4+}(1s^2 3l)$ states for the no screening case and screening cases with $r_d = 12a_0$, $6a_0$ and $2a_0$. The symbols are closed squares for 3s, filled circles for 3p, and filled triangles for 3d.

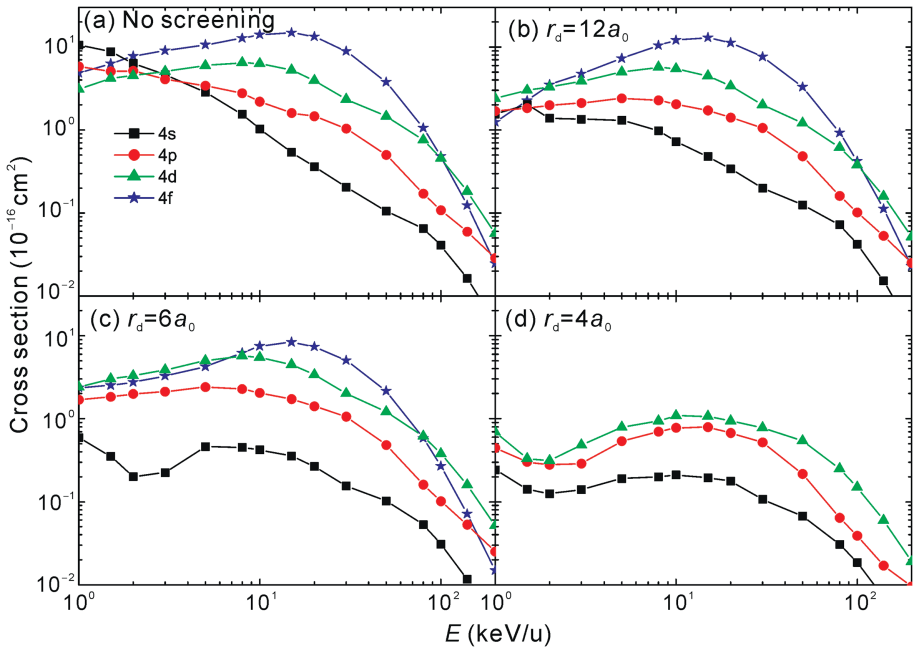

Fig. 4. Energy behavior of state-selective cross sections for electron capture to $N^{4+}(1s^24l)$ states for the no screening case and screening cases with $r_d = 12a_0$, $6a_0$ and $4a_0$. The symbols are closed squares for 4s, filled circles for 4p, filled triangles for 4d, and filled stars for 4f.

for the 4s and 4f states. Those two states are more sensitive to the screening effects due to the positions of nondiabatic interactions. Finally, Fig. 4(d) shows 4s, 4p and 4d cross sections for $r_d = 4a_0$. For this value of r_d the 4f state is already in the continuum. It is worthwhile to note that in this case the magnitude of 4l cross sections are significantly smaller than those of the zero screening case and the energy behavior also differ much from those of other values of r_d and the screening case, because of the extremely decreasing interactions. Meanwhile, the population of 4s, 4p and 4d states show a minimum at the energy of 2 keV/u. The main mechanism of charge transfer processes for the collisions in the low and intermediate energy range is the nonadiabatic interactions and they are very sensitive to the energy difference between the initial and final capture states. As mentioned above, the screening effects make the energy difference decrease. For higher energy collisions, the main mechanism of charge exchange processes is the Coulomb interactions between the electron of target and the projectile ions and the screening effects change these interactions directly. For a given *nl*-state and r_d the effects of the above two mechanisms are different. The competition between these two mechanisms will induce a minimum or maximum in some *nl*-state capture cross sections at some collision energies.

In Fig. 5 we show the 5l capture cross sections as a function of energy for the unscreened case (Fig. 5(a)) and for screened cases with $r_d = 12a_0$, $6a_0$ and $4a_0$, (Fig. 5(b)–(d), respectively). For $r_d = 2a_0$ all 5l states are already in the continuum. Unlike for the 3l states, the 5l electron-capture channel is the subdominant channel for this collision system also in the screened case. It is worthwhile to note that the 5l cross sections show some oscillatory structures in the considered energy range for both the unscreened case and screened cases. This is the consequence of the strong couplings and interferences between 5l states due to the small energy difference between these states. As in the case of capture to 4l states, all 5l partial cross sections for $r_d = 12a_0$ (Fig. 5(b)) are significantly smaller than those of the unscreened case in the low energy region (below 2 keV/u), due to the capture mechanisms discussed above, except for the 5g cross section, which becomes comparable with the corresponding one in the zero-screening case. For $r_d = 6a_0$, the 5g state is absent in the discrete spectrum of N^{4+} ion. Comparing with the high energy region, we can see that the 5l partial cross sections are obviously smaller than those of the unscreened case in the low energy region due to the extended coupling time at these energies. Finally, for $r_d = 4a_0$ only 5s state is still in the discrete spectrum of N^{4+} ion. Due to the decrease exchange coupling matrix with increasing the screening, the magnitude of 5s cross section is significant smaller than the corresponding one in the zero-screening case.

In Fig. 6 we show the energy dependence of partial cross sections for capture to $n = 3$, 4 and 5 (Fig. 6(a)–(c), respectively) shell of N^{4+} ion for $r_d = 12a_0$, $6a_0$, $4a_0$ and $2a_0$ and for the unscreened case. The *n*-partial cross sections for $n = 3$ and $n = 4$, 5 in the considered energy range have quite different behavior when r_d varies. With decreasing r_d the cross sections for capture to $n = 4$ and $n = 5$ decrease, whereas those for $n = 3$ increase in the energy region below 30 keV/u, with the exception of cross section for $r_d = 2a_0$ which above 8 keV/u is larger than that for zero screening. In the energy region above 30 keV/u, the $n = 3$ partial cross section also decrease with decreasing the screening lengths. This behavior of the *n*-capture cross section is obviously direct consequence of the different energy behaviors of *nl* state-selective cross sections when r_d varies, as discussed above for the capture to 3l, 4l and

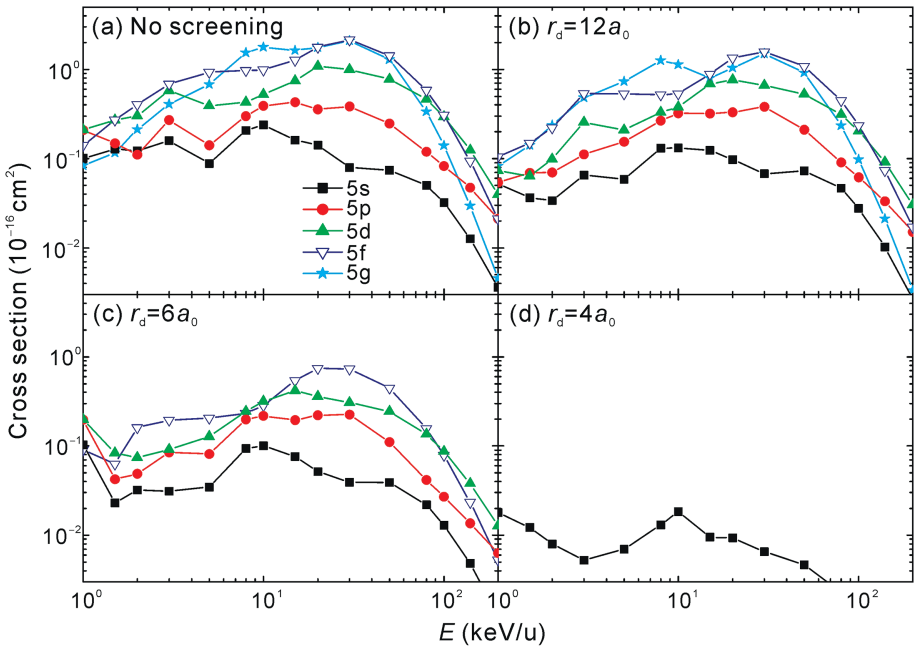

Fig. 5. Energy dependence of state-selective cross sections for electron capture to $N^{4+}(1s^25l)$ states for the no screening case and screening cases with $r_d = 12a_0$, $6a_0$ and $4a_0$. The symbols are closed squares for 5s, filled circles for 5p, filled triangles for 5d, open triangles for 5f, and filled stars for 5g.

5l states of N^{4+} ion (cf. Figs. 3–5). The $n = 3$ capture cross sections increase with decreasing r_d and attain the maximum at $r_d = 4a_0$ in the considered energy region, this is a result of the increased transition probability when the energy difference between the states decreases, as discussed earlier. For $r_d = 2a_0$, the magnitude of $n = 3$ cross section is smaller than that of $r_d = 6a_0$ and $r_d = 4a_0$. This is mainly due to the consequence of the condition for strongest interaction zone with the initial state is fulfilled for the 3l state due to the decrease of energy difference of $N^{4+}(1s^23l)$ and H(1s) states at $r_d = 4a_0$. With increasing the screening ($r_d = 2a_0$), the decrease of energy difference becomes more significant and this makes the interaction between the initial and final states become weak again. The cross sections for all considered screening lengths become smaller than that for the unscreened case in the energy region above 30 keV/u, this is a result of the predominance of the direct exchange coupling between the initial and final states in determining the cross section at high energies and their decrease with decreasing r_d (see Fig. 2). It is worthwhile to note that with increasing the screening, the $n = 3$ state becomes the dominant electron capture channel for this collision system in the considered energy range when $r_d = 4a_0$.

The cross section for capture to $n = 4$ in the screened case with $r_d = 12a_0$ and $6a_0$ is significantly smaller than that in the unscreened case in the energy region below 8 keV/u due to the decreasing of all 4l state-selective cross sections in this energy region [cf. Fig. 4]. For $r_d = 4a_0$ the $n = 4$ cross section is decreased furthermore due to the reduction of electron capture channel. In the $r_d = 4a_0$ case the 4f state is absent in the discrete spectrum of N^{4+}. These arguments apply also to the behavior of $n = 5$ cross sections (Fig. 6(c)). The obvious decrease in the $n = 5$ cross section for $r_d = 4a_0$ in the considered energy range is also due to the reduction in the number of open capture channel. In the $r_d = 4a_0$ case only 5s state is in the discrete spectrum of N^{4+} ion.

The total electron capture cross sections for the unscreened case and for interaction screening with $r_d = 12a_0$, $6a_0$, $4a_0$ and $2a_0$ are shown in Fig. 7 and compared with the results of CTMC calculations of Ref. [10]. For energies above 8 keV/u, the total cross sections in the screened case are smaller than the cross section of the unscreened case and their magnitude decreases with decreasing the screening length. In the energy region below 3 keV/u, the total cross section for $r_d = 4a_0$ is larger than those of other values of screening lengths. In the low energy region, the magnitude and energy behavior of total cross sections for $r_d = 12a_0$ and $r_d = 6a_0$ are determined by the dominant contribution of $n = 4$ and $n = 4$, 5 cross section, respectively, while the cross sections for $r_d = 4a_0$ and $2a_0$ are determined by the contribution from the $n = 3$ partial cross section. It can be seen from this figure that our AOCC cross sections agree well with the CTMC results of Ref. [10] for the unscreened case and screened case with $r_d = 12a_0$ in the 10–100 keV/u energy region, where the CTMC method could be applicable. For the other energy region, the CTMC can not give the high accurate results. For the strong screening cases, the present AOCC cross sections are larger than those of the CTMC calculations [10], because the CTMC is appropriate to treat the strong interactions (hard collisions). This disagreement is mainly due to the fact that CTMC is appropriate to treat the strong interactions (hard collisions), but the screening effects weaken the interactions between the charged particles, and this will make the cross section results from the CTMC method have larger uncertainties.

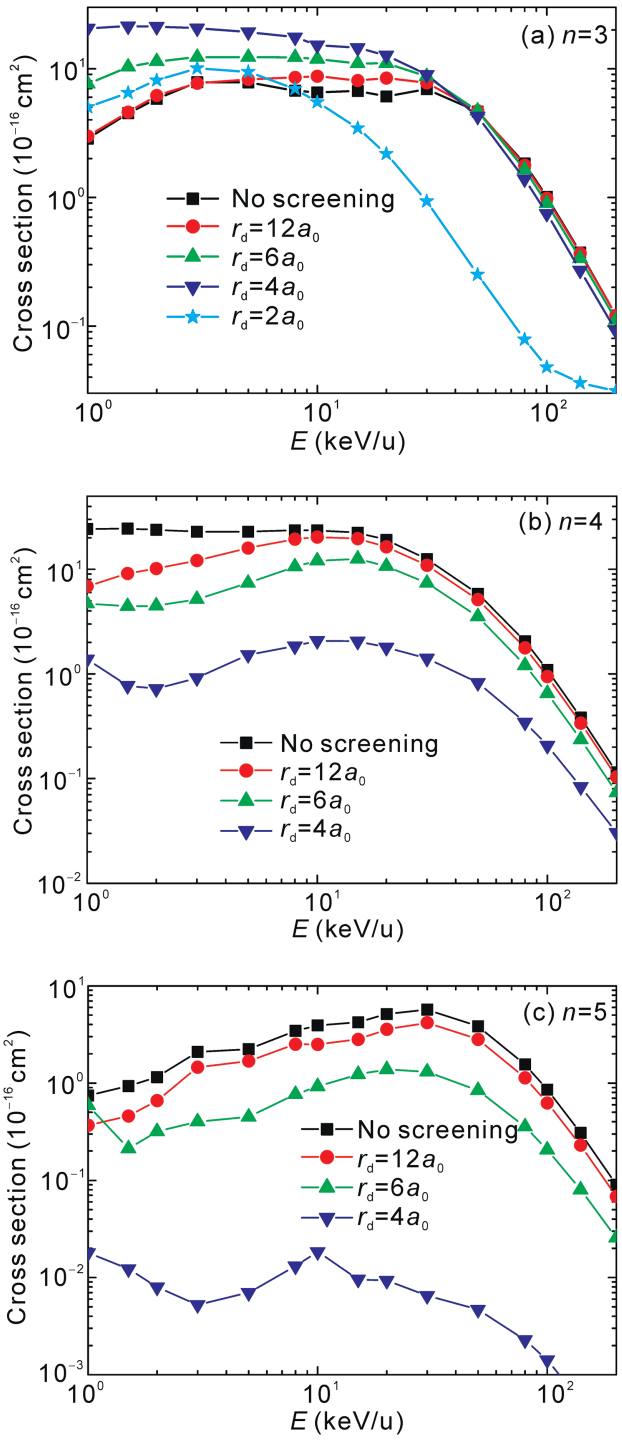

Fig. 6. Energy dependence of partial cross sections for electron capture to $N^{4+}(1s^2nl)$ n = 3, 4, 5 ((a)–(c), respectively) for the unscreened case and screened cases with $r_d = 12a_0$, $6a_0$ and $4a_0$. The symbols are for no screening case (filled squares), $r_d = 12a_0$ (filled circles), $r_d = 6a_0$ (filled up triangles), $r_d = 4a_0$ (filled down triangles), and $r_d = 2a_0$ (filled stars).

3.2. Charge transfer spectral lines

Since the emission from the ion states populated by the electron capture process is an important radiative loss mechanism in hot dense plasmas and since it can serve for diagnostic purpose, it is of considerable interest to investigate the

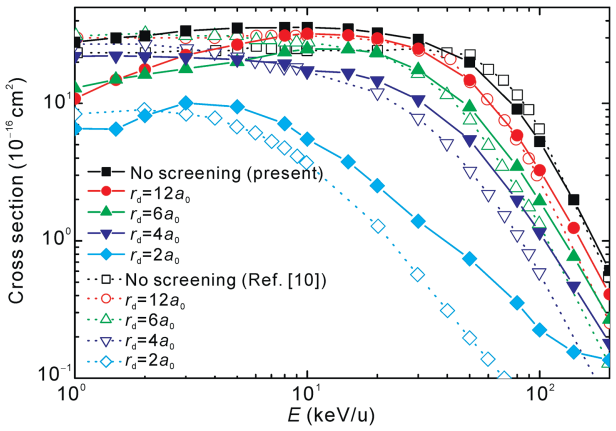

Fig. 7. Total electron capture cross sections for N^{5+}-H collisions with and without screening. The open symbols are the results of Ref. [10].

changes in the spectral line properties due to the interaction screening by the plasma. In the present section, we assume that the population of N^{4+} excited states is determined exclusively by the electron capture from H(1s). The number of the emitted photons per second and cm^3 for the transition $nl \rightarrow n'l'$ can be written as

$$N^{v}_{nl,n'l'} = N^{N^{5+}} N^{H} v B_{nl,n'l'} \left(\sigma_{nl} + \sum_{n''>n} C_{n''l'',nl} \sigma_{n''l''} \right) \tag{12}$$

where $N^{N^{5+}}$ is the density of N^{5+} ions, N^{H} is the density of hydrogen atoms, v is the collision velocity, $C_{n''l'',nl}$ is the cascade matrix, and $B_{nl,n'l'} = A_{nl,n'l'} / \sum_{n''<n} A_{nl,n''l''}$. The radiative transition probabilities $A_{nl,n'l'}$ have been calculated by the wave functions of the Debye–Hückel potential. The spectral lines in plasmas can be broadened by the Doppler, Stark and collisional mechanisms. Here we shall neglect the specific details of the broadening and assume a Gaussian line profile with an arbitrary linewidth Γ. The reduced line intensity then can be defined as

$$I^{v}_{nl\rightarrow n'l'}(E_v) = \left[N^{v}_{nl\rightarrow n'l'} \Big/ \left(N^{N^{5+}} N^{H} \right) \right] \frac{1}{\sqrt{2\pi}\Gamma} \exp\left[-\frac{(E_v - E_{v_0})^2}{\Gamma^2} \right] \tag{13}$$

where $E_{v_0} (= \Delta E_{nl,n'l'})$ is the transition energy.

In Fig. 8(a)–(b) we show the reduced line intensity of Balmer-α line of N^{4+} ion produced by the electron capture at collision energies of 1 and 10 keV/u, respectively, for the unscreened and screened cases with $r_d = 12a_0$, $6a_0$, $4a_0$ and $2a_0$. As we have seen above, the upper 3p state of this transition is not only populated by a direct electron capture transition, but also due to the cascades. The redshifts of the line at the collision energy of 1.0 keV/u for different values of r_d (Fig. 8(a)) don't show a distinct regularity for the reasons mentioned above. The intensity of the line for $r_d = 4a_0$ in Fig. 8(a) is larger than that for the unscreened case because at this energy the 3p-partial cross section is larger than that of the

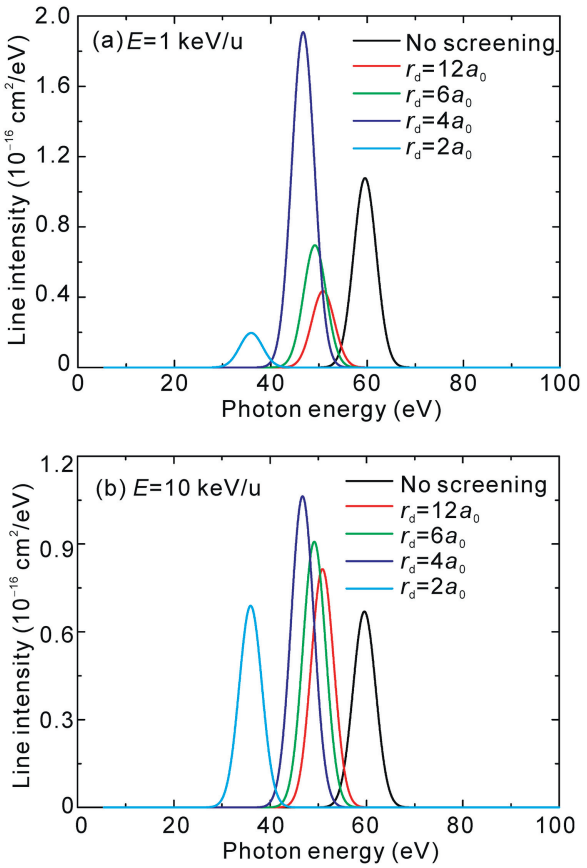

Fig. 8. Reduced line intensity of Balmer-α line of N^{4+} ion, produced by electron capture at collision energies of (a) 1 keV/u and (b) 10 keV/u for the unscreened and screened cases with $r_d = 12a_0$, $6a_0$, $4a_0$ and $2a_0$.

unscreened case. The difference of the line intensities of $r_d = 12a_0$, $6a_0$ and $2a_0$ in Fig. 8(a) is due to the large difference in the 3p capture cross sections at $E = 1.0$ keV/u (a factor of about 10) for these three screening lengths. The Balmer-α intensity for $r_d = 6a_0$ at this collision energy is larger than those of $r_d = 12a_0$ and $2a_0$ also due to the large 3p capture cross sections at this collision energy.

For the collision energy of 10 keV/u, the shifts and intensities of Balmer-α line show quite regular behavior (except for the case of $r_d = 2a_0$): with decreasing r_d the line is increasingly more redshifted with respect to the unscreened interaction value and its intensity increases. For $r_d = 2a_0$, the high excited states have no cascade contributions to 3p state population (only 3s and 3p states are in the discrete spectrum of N^{4+} ion). Due to the large 3p capture cross sections for this value of r_d, the intensity of Balmer-α line is still larger than that of the unscreened case, but its value is smaller than those of the other values of r_d due to the relative small values of 3p capture cross sections and the loss of cascade contributions from $n = 4$ states.

4. Conclusions

We have investigated the electron capture process in N^{5+}-H collisions in a Debye plasma by using the TC-AOCC method in the energy range 1−200 keV/u. The AO expansion basis used in the present study included all the $n \leq 4$ states on H and all the $n \leq 9$ ($l = 0$−5) states on N^{4+} ion and was found to be fully convergent in the energy range considered in both the unscreened and screened cases.

The effects of the interaction screening that have the strong influence on the electron capture dynamics in the N^{5+}-H collision system are the number of remaining bound states in the system for a given value of the screening length, the decrease in exchange couplings with decreasing r_d, and the decrease of energy differences of the states with decreasing r_d. The last of these factors plays a major role in the energy range considered and causes some of the partial cross sections in the screened case to become larger than in the unscreened case. As in the screened case, the dominant contribution to the total capture cross section in the considered energy range gives the $n = 3$ partial cross section. However, while the capture to the $n = 4$ channel in the unscreened case dominates up to the about 20 keV/u, in the screened case the capture to the $n = 4$ is significantly suppressed.

In the present work we have also studied the properties of spectral lines associated with the radiative transitions of captured electrons in the Debye plasma. With respect to the unscreend case, the spectral lines are redshifted, but their intensities strongly depend on the collision energy at which the electron capture takes place, reflecting the energy dependence of *nl*-partial cross section for a given value of the screening length. Since in the considered collision system in the considered energy range the states within the $n = 3$, 4 and 5 manifolds are dominantly populated, the line intensities of transitions between lower states are determined almost exclusively by the cascades populating the upper state of the considered transition. The reduction in the number of bound states in a screened Coulomb potential limits the spectral series to a finite number of lines for a given r_d. Line shifts and series termination are important signatures that can be used in hot dense plasma diagnostics.

Acknowledgment

This work was supported by the National Basic Research Program of China (Grant No. 2013CB922200), by the National Natural Science Foundation of China (Grant Nos. 11204017, 11474033 and 11474032) and by the foundation for the development of Science and Technology of China Academy of Engineering Physics (Grant No. 2013A0102005).

References

[1] D. Dijkkamp, D. Ćirić, F.J. Heer, Total capture and line-emission cross sections for C^{6+}-, N^{7+}-, O^{8+}-H collisions in the energy range 3−7.5 keV/u, Phys. Rev. Lett. 54 (1985) 1004.

[2] F.W. Meyer, A.M. Howald, C.C. Havener, R.A. Phaneuf, Low-energy total-electron-capture cross sections for fully stripped and H-like projectiles incident on H and H_2, Phys. Rev. A 32 (1985) 3310.

[3] W. Fritsch, C.D. Lin, Atomic-orbital-expansion studies of electron transfer in bare-nucleus Z(Z = 2,4−8)—hydrogen-atom collisions, Phys. Rev. A 29 (1984) 3039.

[4] R.K. Janev, L.P. Presnyakov, V.P. Shevelko, Physics of Highly Charged Ions, Springer, Berlin, 1985.
[5] Patricia Barragán, Le Anh-Thu, C.D. Lin, Hyperspherical close-coupling calculations for electron-capture cross sections in low-energy Ne^{10+}+H(1s) collisions, Phys. Rev. A 74 (2006) 012720.
[6] K. Scheibner, J.C. Weisheit, N.F. Lane, Plasma screening effects on proton-impact excitation of positive ions, Phys. Rev. A 35 (1987) 1252.
[7] C.-G. Kim, Y.-D. Jung, Semiclassical electron capture probabilities for proton–hydrogenic ion collisions in dense plasmas, Phys. Plasmas 5 (1998) 2806;
Dynamic plasma screening effects on semiclassical electron captures from hydrogenic ions by protons in weakly coupled plasmas, Phys. Plasmas 5 (1998) 3493.
[8] Y.-D. Jung, Plasma screening effects on resonant charge transfer in strongly coupled plasmas, Europhys. Lett. 69 (2005) 753.
[9] H. Zhang, J.G. Wang, B. He, Y.B. Qiu, R.K. Janev, Charge exchange and ionization in hydrogen atom-fully stripped ion collisions in Debye plasmas, Phys. Plasmas 14 (2007) 053505.
[10] M.K. Pandey, Y.-C. Lin, Y.K. Ho, Investigation of charge transfer and ionization in He-like systems (Li^+, Be^{2+}, B^{3+}, C^{4+}, N^{5+}, O^{6+})-hydrogen atom collisions in Debye plasmas, Phys. Plasmas 20 (2013) 022104.
[11] S.L. Zeng, L. Liu, J.G. Wang, R.K. Janev, Atomic collisions with screened Coulomb interactions: excitation and electron capture in H^+ + H collisions, J. Phys. B 41 (2008) 135202.
[12] L. Liu, J.G. Wang, R.K. Janev, Dynamics of He^{2+}+H(1s) excitation and electron-capture processes in Debye plasmas, Phys. Rev. A 77 (2008) 032709.
[13] L. Liu, J.G. Wang, R.K. Janev, Dynamics of He^{2+}+H(1s) ionization with screened Coulomb interactions, Phys. Rev. A 77 (2008) 042712.
[14] L. Liu, J.G. Wang, R.K. Janev, Polarization spectroscopy of $He^+(nl)$ produced in collisions of He^{2+} with H in Debye plasmas, Phys. Rev. A 83 (2011) 012712.
[15] L. Liu, J.G. Wang, R.K. Janev, Dynamics of O^{8+}+H electron capture in Debye plasmas, Phys. Rev. A 79 (2009) 052702.
[16] E.J. Shipsey, J.C. Browne, R.E. Olson, Electron capture and ionisation in C^{5+}, N^{5+}, O^{6+}+H collisions, J. Phys. B 14 (1981) 869.
[17] M. Bendahman, S. Bliman, S. Dousson, D. Hitz, R. Gayet, et al., Electron capture from atomic hydrogen by multiply charged ions in low energy collisions, J. Phys. Paris. 46 (1985) 561.
[18] M. Gargaud, R. McCarroll, Charge transfer in low-energy collisions of N^{3+}, C^{4+} and N^{5+} with H and H^2, J. Phys. B 18 (1985) 463.
[19] J. Hanssen, R. Gayet, C. Harel, A. Salin, Electron capture by C^{4+}, N^{5+} and O^{6+} from atomic hydrogen in the keV amu^{-1} energy range, J. Phys. B 17 (1984) L323.
[20] C. Harel, H. Jouin, Electron capture by slow multicharged ions: core effect on final 1 distributions, J. Phys. B 21 (1988) 859.
[21] N. Shimakura, M. Kimura, Electron capture in collisions of N^{5+} ions with H atoms from the meV to keV energy regions, Phys. Rev. A 44 (1991) 1659.
[22] M. Purkait, A. Dhara, S. Sounda, C.R. Mandal, Inelastic processes in the interactions of partially stripped ions of carbon, nitrogen and oxygen with atomic hydrogen at intermediate and high energies, J. Phys. B 34 (2001) 755.
[23] S. Sounda, A. Dhara, M. Purkait, C.R. Mandal, State selective electron capture in partially stripped ion-atom interaction at intermediate and high energies, Eur. Phys. J. D 38 (2006) 257.
[24] J. Kuang, C.D. Lin, Convergent TCAO close-coupling calculations for electron transfer, excitation and ionization in intermediate keV He^{2+}-H collisions, J. Phys. B 30 (1997) 101.
[25] C.M. Reeves, Use of Gaussian functions in the calculation of wave-functions for small molecules. I. Preliminary investigations, J. Chem. Phys. 39 (1963) 1.
[26] G. Peach, H.E. Saraph, M.J. Seaton, Atomic data for opacity calculations. IX. The lithium isoelectronic sequence, J. Phys. B 21 (1988) 3669.
[27] L. Liu, J.G. Wang, R.K. Janev, State-selective electron capture in N^{5+}-H and O^{6+}-H collisions, J. Phys. B 45 (2012) 015202.
[28] D. Dijkkamp, D. Ćirić, E. Vlieg, A. de Boer, F.J. de Heer, Subshell-selective electron capture in collisions of C^{4+}, N^{5+}, O^{6+} with H, H_2 and He, J. Phys. B 18 (1985) 4763.
[29] R.A. Phaneuf, F.W. Meyer, Single-electron capture by multiply charged ions of carbon, nitrogen, and oxygen in atomic and molecular hydrogen, Phys. Rev. A 17 (1978) 534.